# Gradient Direction for Screen Content Image Quality Assessment

Zhangkai Ni, Lin Ma, *Member, IEEE*, Huanqiang Zeng, *Member, IEEE*, Canhui Cai, *Senior Member, IEEE*, and Kai-Kuang Ma, *Fellow, IEEE*

***Abstract*—In this letter, we make the first attempt to explore the usage of the *gradient direction* to conduct the perceptual quality assessment of the *screen content images* (SCIs). Specifically, the proposed approach first extracts the gradient direction based on the local information of the image gradient magnitude, which not only preserves gradient direction consistency in local regions, but also demonstrates sensitivities to the distortions introduced to the SCI. A deviation-based pooling strategy is subsequently utilized to generate the corresponding image quality index. Moreover, we investigate and demonstrate the complementary behaviors of the gradient direction and magnitude for SCI quality assessment. By jointly considering them together, our proposed SCI quality metric outperforms the state-of-the-art quality metrics in terms of correlation with human visual system perception.[1]**

***Index Terms*—Human visual system, gradient direction, image quality assessment, screen content image (SCI).**

## I. Introduction

With the rapid development of the Internet and wireless communications, *screen content images* (SCIs) [1]–[3] are prevalent in various scientific and social media. Unlike natural images captured by video cameras, SCIs are generated by computers or other electronic devices. The image content of a typical SCI consists of a mixture of natural images, texts, charts, logos, graphics, and so on. As a result, SCIs could possess some special features or characteristics (e.g., sharp edges) that are very different from that of natural images. Therefore, the way to assess the quality or distortion of natural images will not be necessarily all applicable to SCIs. In this letter, it is our goal to investigate this issue and propose an objective *image quality assessment* (IQA) for SCIs. That is, the quantitative measurement yielded by the proposed metric should be highly consistent with the subjective judgment made by the *human visual system* (HVS).

In the past, *mean square error* (MSE) and *peak signal-to-noise ratio* (PSNR) have been widely deployed to conduct objective measurement for assessing the visual quality of natural images. However, it is also well-known that they are not highly consistent with the judgment made by the HVS. Therefore, many IQA metrics have been proposed by taking the HVS characteristics into account [1]–[16]. Among them, the well-known *structural similarity* (SSIM) [10] and its variants (e.g., multiscale SSIM, denoted as MS-SSIM [11]) are good examples. Both utilize image structure to develop the IQA metrics, since the HVS is highly sensitive to the image structure inherited in images. On the pooling stage for computing the overall score, however, both SSIM and MS-SSIM take the mean value of the local quality values, which is considered not accurate due to the fact that different image regions should contribute the overall perception of the image's quality through different ways [12]–[14].

A promising approach on the development of the IQA metrics for natural images lies in the use of the image gradient [15]. For that, Zhang *et al.* [12] proposed to compute the phase congruency as the main feature and the gradient magnitude as its complementary feature for generating the final objective score. Liu *et al.* [13] used the *gradient similarity* to capture both contrast and structural changes as the main information to measure the image quality. Chen *et al.* [16] proposed the so-called *gradient-based SSIM* (GSSIM), which specifically addresses the issue when the natural images under evaluation are severely blurred. Zhu *et al.* [17] proposed an IQA model by measuring the gradient similarity across multiple-scale framework, with intrascale and interscale pooling. Xue *et al.* [18] combined the normalized gradient magnitude with the Laplacian of Gaussian to form the joint statistics of local contrast features to compute the perceptual quality score.

Although the gradient information has shown its promising usage for assessing the perceptual quality of natural images [12], [13], [16], [18], [19], it often fails to reflect the visual quality of SCIs with reasonable accuracy [1], [3]. This is because the characteristics of SCIs are quite different from that of natural images. The common practice of the existing methods (e.g., [12], [13], [16], [18], [19]) is to exploit the gradient magnitude to generate various features, while the gradient direction

Manuscript received March 21, 2016; revised June 23, 2016; accepted July 28, 2016. Date of publication August 10, 2016; date of current version August 26, 2016. This work was supported in part by the National Natural Science Foundation of China under the Grant 61372107 and Grant 61401167, in part by the Natural Science Foundation of Fujian Province under the Grant 2016J01308, in part by the Opening Project of State Key Laboratory of Digital Publishing Technology under the Grant FZDP2015-B-001, in part by the Zhejiang Open Foundation of the Most Important Subjects, in part by the High-Level Talent Project Foundation of Huaqiao University under the Grant 14BS201 and Grant 14BS204, and in part by the Graduate Student Scientific Research Innovation Project Foundation of Huaqiao University. The associate editor coordinating the review of this manuscript and approving it for publication was Prof. Joao M. Ascenso. *(Corresponding author: Huanqiang Zeng).*

Z. K. Ni, H. Q. Zeng, and C. H. Cai are with the School of Information Science and Engineering, Huaqiao University, Xiamen 361021, China (e-mail: ddkklove@gmail.com; zeng0043@hqu.edu.cn; chcai@hqu.edu.cn).

L. Ma is with Huawei Noah's Ark Lab, Hong Kong (e-mail: forest.linma@gmail.com).

K.-K. Ma is with the School of Electrical and Electronic Engineering, Nanyang Technological University, 639798 Singapore (e-mail: ekkma@ntu.edu.sg).

Color versions of one or more of the figures in this letter are available online at http://ieeexplore.ieee.org.

Digital Object Identifier 10.1109/LSP.2016.2599294

[1]The source code for the proposed SCI quality metric will be available at http://www.ee.cuhk.edu.hk/~lma/welcome_files/SCI_GSS.html.

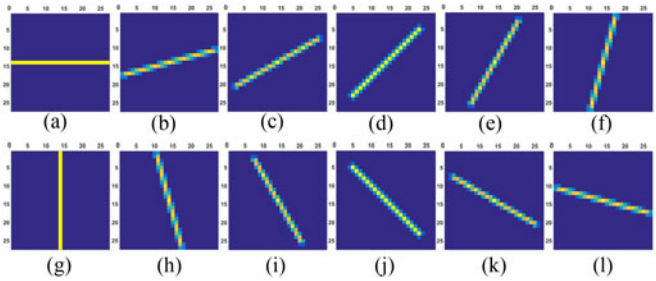


Fig. 1. Convolution kernels of twelve different directions, from 0 to $\pi$ with a step-size of $\frac{\pi}{12}$.

is mostly neglected. Although Zhu *et al.* [17] has considered the gradient direction on their developed metric, their proposed metric is for assessing natural images, besides the computation of gradient direction and its associated similarity measurement are all different from ours.

In this letter, a simple yet efficient approach by exploring the similarity of gradient direction for SCI quality assessment is proposed based on the observation that the gradient direction can significantly reflect the quality perception of SCIs. The computation of gradient direction is based on the finding of which direction has incurred the largest possible variation over the gradient magnitude field. Furthermore, a gradient direction-similarity measurement method is also proposed. Together with the gradient magnitude, an accurate IQA metric for SCIs is then developed, which outperforms the state-of-the-art SCI quality metrics.

The rest of this letter is organized as follows. Section II introduces the proposed gradient direction for SCI quality assessment. Section III presents the experimental results and comparisons. Section IV concludes this letter.

## II. Gradient Direction for SCI Quality Assessment

### A. Gradient Direction

The gradient direction of an SCI is computed under a fixed direction, and the computation is performed at each pixel location $(x, y)$, respectively. In our approach, 12 directions, ranging from 0 to $\pi$ with a step size of $\frac{\pi}{12}$ (i.e., $i \times \frac{\pi}{12}, i \in \{0, \ldots, 11\}$), are considered. As a result, there are 12 gradient direction maps $D_i$ for each SCI under consideration. Each $D_i(x, y)$ is obtained by conducting a convolution of the gradient magnitude field of the input SCI (denoted as $G(x, y)$) with a convolution kernel $\mathscr{L}_i$ at the $i$th direction, as shown in Fig. 1. That is

$$D_i(x, y) = \mathscr{L}_i \otimes G(x, y) \tag{1}$$

where $G(x, y)$ is the gradient magnitude of the input SCI at location $(x, y)$, which can be computed as

$$G(x, y) = |G_H(x, y)| + |G_V(x, y)| \tag{2}$$

where the symbol $|\cdot|$ denotes the absolute value of the indicated quantity. Let $I(x, y)$ denote the luminance component of each given SCI. $G_H$ and $G_V$ are, respectively, the approximate values of the directional derivatives on the input SCI in the horizontal and vertical directions and can be computed as follows:

$$\begin{aligned} G_H(x, y) &= I(x + 1, y) - I(x, y) \\ G_V(x, y) &= I(x, y + 1) - I(x, y). \end{aligned} \tag{3}$$

As shown in Fig. 1, each convolution kernel $\mathscr{L}_i$ is a line segment at the $i$-th direction ($i \times \frac{\pi}{12}, i \in \{0, \ldots, 11\}$). Each $\mathscr{L}_i$ can be obtained by rotating the convolution kernel $\mathscr{L}_0$ with the angle $i \times \frac{\pi}{12}$. "$\otimes$" denotes the convolution operator. Equation (1) is to convolve the gradient magnitude $G$ with the $i$-th direction filter $\mathscr{L}_i$ to form the corresponding gradient direction map $D_i$. With $\mathscr{L}_i$ convolving $G$, the gradient direction responses will not fluctuate dramatically as the commonly used $\arctan(\frac{G_V}{G_H})$, especially in the smooth regions, as the local neighboring pixels are taken into consideration. Consequently, the resulted gradient direction map $D_i$ will be able to preserve gradient direction consistency in local regions. After obtaining the gradient direction maps for all the 12 directions, the final gradient direction map $D$ for the input SCI is generated by selecting the maximum value among the responses over all directions

$$D(x, y) = n \times \frac{\pi}{12}, \text{where } n = \arg\max_i \{D_i(x, y)\}, \quad i \in \{0, \ldots, 11\}. \tag{4}$$

To further verify the effectiveness of the proposed gradient direction on SCI quality perception, extensive experiments have been conducted to obtain the comparisons of the gradient direction distributions between various typical SCIs and their corresponding distorted SCIs with different kinds of distortions. Due to the limited space, Fig. 2 demonstrates an example of SCI with Gaussian blurring, motion blurring, contrast change. The blue bars denote the gradient direction distributions of the corresponding SCIs, while the red bars indicate the difference between the original and distorted SCIs. One can see that for the distorted SCIs by Gaussian blurring and motion blurring, the smoothing effect introduced by blurring significantly increases the distribution at the horizontal direction and decreases the distribution at the vertical direction. For the distorted SCI by contrast change, all the pixel values are modified to alter the contrast information, which tends to change the distributions at all directions. Hence, it can be clearly observed from Fig. 2 that the proposed gradient direction can effectively reflect the perceptual quality degradation caused by Gaussian blurring, motion blurring, and contrast change. Note that similar observations can be found in other SCIs with different kinds of distortions, such as Gaussian noise, compression artifacts, etc. Hence, the proposed gradient direction is explored as an effective predictive factor for SCI quality assessment in this letter.

### B. Gradient Direction Similarity

By performing the proposed gradient direction on the reference and distorted SCIs to obtain the corresponding gradient direction maps, their gradient direction similarity map (denoted as DS) can be computed as follows:

$$\mathrm{DS}(x, y) = \frac{2D_r(x, y)D_d(x, y) + c_D}{D_r^2(x, y) + D_d^2(x, y) + c_D} \tag{5}$$


Fig. 2. SCIs and the corresponding direction distributions. (a) Original SCI; (b)–(d) are the corresponding distorted versions with Gaussian blurring, motion blurring, contrast change, respectively; (e)–(h) are the corresponding gradient direction distributions of (a)–(d) (blue bars) and the distribution differences between original SCI and distorted versions (red bars).

where $D_r$ and $D_d$ are the gradient direction maps of the reference and distorted SCIs, respectively, $c_D$ is a small positive constant to avoid instability.

The gradient similarity map DS indicates the local quality map by considering the gradient direction information. In order to generate the final quality score of the distorted SCI, a pooling process on DS is needed. As different regions may contribute differently to the overall perception of an image's quality, a new deviation pooling strategy is employed to produce the final gradient direction similarity score DSS.

$$\mathrm{DSS} = \left( \frac{1}{N} \sum_{(x,y)\in\Omega} \left( \mathrm{DS}(x,y) - m_{\mathrm{DS}} \right)^2 \right)^{\frac{1}{2}} \tag{6}$$

where $\Omega$ denotes all the pixels within the SCI. $N$ is the number of pixels in $\Omega$. $m_{\mathrm{DS}}$ is the mean value of DS. Note that a larger value of DSS represents a larger distortion range, indicating a lower SCI perceptual quality.

### C. Incorporating Gradient Direction With Magnitude

The gradient magnitude is commonly used for evaluating the natural image perceptual quality [12], [13], [16], [18], which could be considered as a complementary part to the proposed gradient direction. Based on this intuition, they can be jointly utilized to describe the perceptual quality degradation of SCI. Similar to the proposed gradient direction similarity DS shown in (5), we propose the following measurement to evaluate the gradient magnitude similarity (denoted as MS) between the reference and distorted SCIs

$$\mathrm{MS}(x,y) = \frac{2G_r(x,y)G_d(x,y) + c_M}{G_r^2(x,y) + G_d^2(x,y) + c_M} \tag{7}$$

where $G_r$ and $G_d$ are the gradient magnitude maps of the reference and distorted SCIs computed by (2), respectively, and $c_M$ is a small positive constant to ensure the numerical stability.

As aforementioned, DS and MS are computed to depict the SCI similarity from different perspectives. In order to fully depict the SCI similarity, DS and MS are fused together as

$$\mathrm{GS}(x,y) = [\mathrm{DS}(x,y)]^{\alpha} \cdot [\mathrm{MS}(x,y)]^{\beta} \tag{8}$$

where GS is the fused gradient similarity map, $\alpha \geq 0$ and $\beta \geq 0$ are two parameters used to adjust the relative importance of the proposed gradient direction and gradient magnitude, respectively. By setting $\alpha = 0$, only the gradient magnitude is employed for quality assessment, while only the gradient direction is considered when $\beta = 0$. In this study, we set $\alpha = \beta = 1$ to simplify the expression by regarding gradient direction and gradient magnitude as the same importance.

Furthermore, the fused gradient similarity map GS is pooled together to generate the quality index GSS, which indicates the perceptual quality of the distorted SCI

$$\mathrm{GSS} = \left( \frac{1}{N} \sum_{(x,y)\in\Omega} \left( \mathrm{GS}(x,y) - m_{\mathrm{GS}} \right)^2 \right)^{\frac{1}{2}} \tag{9}$$

where $m_{\mathrm{GS}}$ is the mean value of GS. Similar to DSS, the higher the GSS score, the larger the distortion range, and thus, the lower the SCI perceptual quality.

## III. Experimental Results and Discussions

### A. Database and Evaluation Criteria

To our best knowledge, SIQAD [3] is the only public available SCI database. It consists of 980 distorted SCIs that are generated from 20 reference SCIs under seven types of distortions; i.e., the Gaussian noise (GN), Gaussian blur (GB), motion blur (MB), contrast change (CC), JPEG compression, JPEG2000 compression, and layer segmentation based coding (LSC). For each of these distortion category, seven different degradation levels are considered.

To conduct a meaningful and fair comparsion, a normalization process is first performed on all quality metrics under consideration. For that, a logarithmic mapping function is employed to fit the output from each quality metric and its subjective scores [20]. After normalization, three commonly used

TABLE I
PERFORMANCE COMPARISONS BETWEEN THE PROPOSED AND OTHER IQA METRICS BASED ON THE MEASUREMENT OF PLCC, SROCC, AND RMSE

| | Distortions | PSNR | SSIM | MSSIM | IWSSIM | VIF | IFC | VSNR | MAD | FSIM | GSIM | GMSD | VSI | DSS | MSS | GSS |
|---|---|---|---|---|---|---|---|---|---|---|---|---|---|---|---|---|
| PLCC | GN | 0.9053 | 0.8806 | 0.8783 | 0.8804 | 0.9011 | 0.8791 | 0.8840 | 0.8852 | 0.7428 | 0.8448 | 0.8956 | 0.8762 | 0.8240 | 0.8933 | 0.8645 |
| | GB | 0.8603 | 0.9014 | 0.8984 | 0.9079 | 0.9102 | 0.9061 | 0.8890 | 0.9120 | 0.7206 | 0.8831 | 0.9094 | 0.8502 | 0.8850 | 0.9042 | 0.9073 |
| | MB | 0.7044 | 0.8060 | 0.8240 | 0.8414 | 0.8490 | 0.6782 | 0.7829 | 0.8361 | 0.6874 | 0.7711 | 0.8436 | 0.6620 | 0.7666 | 0.8541 | 0.8314 |
| | CC | 0.7401 | 0.7435 | 0.8371 | 0.8404 | 0.7076 | 0.6870 | 0.7667 | 0.3933 | 0.7507 | 0.8077 | 0.7827 | 0.7723 | 0.2678 | 0.7798 | 0.6091 |
| | JPEG | 0.7545 | 0.7487 | 0.7756 | 0.7998 | 0.7986 | 0.7606 | 0.7972 | 0.7662 | 0.5566 | 0.6778 | 0.7746 | 0.7124 | 0.7135 | 0.7923 | 0.7948 |
| | J2K | 0.7893 | 0.7749 | 0.7951 | 0.8040 | 0.8205 | 0.7963 | 0.8170 | 0.8344 | 0.6675 | 0.7242 | 0.8509 | 0.7479 | 0.7021 | 0.8308 | 0.8130 |
| | LSC | 0.7805 | 0.7307 | 0.7729 | 0.8155 | 0.8385 | 0.7679 | 0.7982 | 0.8184 | 0.5964 | 0.7218 | 0.8559 | 0.7454 | 0.6909 | 0.8235 | 0.8084 |
| | Overall | 0.5869 | 0.7561 | 0.6161 | 0.6527 | **0.8198** | 0.6395 | 0.5982 | 0.6191 | 0.5389 | 0.5663 | 0.7387 | 0.5543 | 0.7687 | 0.7846 | **0.8461** |
| SROCC | GN | 0.8790 | 0.8694 | 0.8679 | 0.8743 | 0.8888 | 0.8717 | 0.8662 | 0.8721 | 0.7373 | 0.8404 | 0.8856 | 0.8655 | 0.8207 | 0.8829 | 0.8521 |
| | GB | 0.8573 | 0.8921 | 0.8883 | 0.9060 | 0.9059 | 0.9106 | 0.8827 | 0.9087 | 0.7286 | 0.8796 | 0.9119 | 0.8495 | 0.8847 | 0.9106 | 0.9053 |
| | MB | 0.7130 | 0.8041 | 0.8238 | 0.8421 | 0.8492 | 0.6737 | 0.7799 | 0.8357 | 0.6641 | 0.7753 | 0.8441 | 0.7658 | 0.7804 | 0.8715 | 0.8397 |
| | CC | 0.6828 | 0.6405 | 0.7506 | 0.7563 | 0.6433 | 0.6396 | 0.6694 | 0.3907 | 0.7175 | 0.7148 | 0.6378 | 0.6495 | 0.1154 | 0.6553 | 0.5974 |
| | JPEG | 0.7569 | 0.7576 | 0.7787 | 0.7978 | 0.7924 | 0.7636 | 0.8084 | 0.7674 | 0.5879 | 0.6796 | 0.7712 | 0.7196 | 0.7137 | 0.7909 | 0.7969 |
| | J2K | 0.7746 | 0.7603 | 0.7855 | 0.7998 | 0.8131 | 0.7980 | 0.8112 | 0.8382 | 0.6363 | 0.7125 | 0.8436 | 0.7299 | 0.6962 | 0.8348 | 0.8141 |
| | LSC | 0.7930 | 0.7371 | 0.7711 | 0.8214 | 0.8463 | 0.7713 | 0.8088 | 0.8154 | 0.5979 | 0.7145 | 0.8592 | 0.7419 | 0.6867 | 0.8421 | 0.8164 |
| | Overall | 0.5604 | 0.7566 | 0.6115 | 0.6545 | 0.8065 | 0.6011 | 0.5743 | 0.6067 | 0.5279 | 0.5551 | 0.7305 | 0.5381 | 0.7180 | **0.8194** | **0.8359** |
| RMSE | GN | 6.3372 | 7.0679 | 7.1309 | 7.7044 | 6.4673 | 7.1096 | 6.9721 | 6.9391 | 9.9860 | 7.9811 | 6.6354 | 7.1890 | 8.452 | 6.704 | 7.497 |
| | GB | 7.7376 | 6.5701 | 6.6638 | 6.3619 | 6.2859 | 6.4193 | 6.9506 | 6.2269 | 10.5230 | 7.1210 | 6.3111 | 7.9900 | 7.066 | 6.483 | 6.383 |
| | MB | 9.2287 | 7.6967 | 7.3675 | 7.0260 | 6.8704 | 9.5544 | 8.0897 | 7.1322 | 9.4432 | 8.2788 | 6.9816 | 9.7450 | 8.349 | 6.763 | 7.225 |
| | CC | 8.4591 | 8.4116 | 6.8818 | 6.8184 | 8.8876 | 9.1407 | 8.0760 | 11.5652 | 8.3190 | 7.4160 | 7.8294 | 7.9900 | 9.852 | 7.875 | 9.976 |
| | JPEG | 6.1665 | 6.2295 | 5.9311 | 5.6406 | 5.6551 | 6.1004 | 5.6726 | 6.0380 | 7.8072 | 6.9085 | 5.9427 | 6.5950 | 6.584 | 5.733 | 5.702 |
| | J2K | 6.3819 | 6.5691 | 6.3040 | 6.1804 | 5.9412 | 6.2875 | 5.9929 | 5.7276 | 7.7404 | 7.1675 | 5.4591 | 6.8990 | 7.401 | 5.785 | 6.051 |
| | LSC | 5.3336 | 5.8253 | 5.4141 | 4.9379 | 4.6497 | 5.4657 | 5.1429 | 4.9025 | 6.8486 | 5.9046 | 4.4121 | 5.6880 | 6.168 | 4.840 | 5.022 |
| | Overall | 11.5898 | 9.3676 | 11.2744 | 10.8444 | **8.1969** | 11.0048 | 11.4706 | 11.2409 | 12.0583 | 11.7980 | 9.6484 | 11.9150 | 9.156 | 8.874 | **7.631** |

The test SCIs are drawn from the database SIQAD [3]. The top two performances are highlighted in boldface.

criteria, i.e., *Pearson linear correlation coefficient* (PLCC), *Spearman rank order correlation coefficient* (SROCC), and *root mean squared error* (RMSE), are used to evaluate the prediction accuracy, prediction monotonicity, and prediction consistency, respectively [14], [21]–[24]. For PLCC and SROCC, the higher the value, the better the performance in terms of correlation with the human perception. For RMSE, on the other hand, the lower the value, the better the performance.

In order to demonstrate the performance of the proposed algorithm, several state-of-the-art IQA metrics are compared, including PSNR, SSIM [10], MSSIM [11], IWSSIM [25], VIF [21], IFC [22], VSNR [26], MAD [27], FSIM [12], GSIM [13], GMSD [14], and VSI [28].

### *B. Performance Comparisons*

Table I lists the PLCC, SROCC, and RMSE values of the proposed and other IQA metrics using the test SCIs drawn from the database SIQAD. Overall, GSS performs the best as the objective measurement from this metric is mostly consistent with the subjective judgment made by the HVS. The performance of the VIF metric is the second best. Compared with the other metrics based on the gradient magnitude (e.g., GSIM and GMSD), our proposed GSS witnesses an evident advantage that the gradient direction plays an important role for SCI quality assessment. And the success of GSS actually stems from the complementary behavior of the gradient direction to the gradient magnitude.

To more clearly demonstrate an IQA model's ability in predicting SCI quality degradations caused by certain types of distortions, we also calculate PLCC, SROCC, and RMSE values for each distortion type. It can be seen that the proposed GSS performs competitively on the first three distortions, i.e., GN, GB, and MB. Meanwhile, for the distortion of CC, the proposed GSS does not perform very well. This is because CC only affects the intensity of image rather than the image structures [4], which the proposed GSS cannot well describe.

Moreover, we examine the performances of the gradient direction and magnitude, respectively, for measuring the SCI perceptual quality. By assigning different values to $\alpha$ and $\beta$ in (8), we can obtain the quality metrics by considering only gradient direction ($\beta = 0$) or gradient magnitude ($\alpha = 0$). It can be observed that both direction similarity score DSS and magnitude similarity score MSS achieve relatively better performances than previous IQA metrics. Since gradient magnitude conveys the local image brightness variations, while the gradient direction carries rich spatial information even in the areas where intensities change gradually, the gradient direction and magnitude play complementary roles to capture the edge properties for high contributions to SCI quality assessment. Consequently, by considering the gradient direction and magnitude together, the proposed GSS performs the best and surpasses the state-of-the-art competitor models.

## IV. CONCLUSION

In this letter, we comprehensively investigate the gradient direction for SCI quality assessment. More specifically, by using the local information of the image gradient magnitude, a novel gradient direction computation method together with a deviation-based pooling strategy is presented to accurately reflect the perceptual quality degradations of SCIs. Furthermore, the proposed gradient direction and gradient magnitude are demonstrated to play complementary roles for SCI quality assessment. Experimental results on public SCI quality assessment database have shown the effectiveness and superiority of the proposed SCI quality metric.

## REFERENCES


[1] S. Wang, K. Gu, K. Zeng, Z. Wang, and W. Lin, "Perceptual screen content image quality assessment and compression," *IEEE Int. Conf. Image Process.*, Sep. 2015, pp. 1434–1438.

[2] S. Shi, X. Zhang, S. Wang, R. Xiong, and S. Ma, "Study on subjective quality assessment of screen content images," *Pict. Coding Symp.*, , 2015, pp. 75–79.

[3] H. Yang, Y. Fang, and W. Lin, "Perceptual quality assessment of screen content images," *IEEE Trans. Image Process.*, vol. 24, no. 11, pp. 4408–4421, Aug. 2015.

[4] S. Wang *et al.*, "A patch-structure representation method for quality assessment of contrast changed images," *IEEE Signal Process. Lett.*, vol. 22, no. 12, pp. 2387–2390, Oct. 2015.

[5] L. Ma, S. Li, F. Zhang, and K. N. Ngan, "Reduced-reference image quality assessment using reorganized DCT-based image representation," *IEEE Trans. Multimedia*, vol. 13, no. 4, pp. 824–829, Aug. 2011.

[6] R. Soundararajan and A. C. Bovik, "RRED Indices: Reduced reference entropic differencing for image quality assessment," *IEEE Trans. Image Process.*, vol. 21, no. 2, pp. 517–526, Feb. 2012.

[7] L. Ma, W. Lin, C. Deng, and K. N. Ngan, "Image retargeting quality assessment: A study of subjective scores and objective metrics," *IEEE J. Sel. Topics Signal Process.*, vol. 6, no. 6, pp. 626–639, Oct. 2012.

[8] L. Ma, S. Li, and K. N. Ngan, "Reduced-reference image quality assessment in reorganized DCT domain," *Signal Process., Image Commun.*, vol. 28, no. 8, pp. 884–902, Aug. 2013.

[9] A. Mittal, A. Moorthy, and A. Bovik, "No-reference image quality assessment in the spatial domain," *IEEE Trans. Image Process.*, vol. 21, no. 12, pp. 4695–4708, Dec. 2012.

[10] Z. Wang, A. C. Bovil, H. R. Sheikh, and E. P. Simoncelli, "Image quality assessment: From error visibility to structural similarity," *IEEE Trans. Image Process.*, vol. 13, no. 4, pp. 600–612, Apr. 2004.

[11] Z. Wang, E. P. Simoncelli, and A. C. Bovil, "Multi-Scale structural similarity for image quality assessment," *in Proc. IEEE Conf. Signals, Syst. Comput.*, vol. 2, Nov. 2003, pp. 1398–1402.

[12] L. Zhang, L. Zhang, X. Mou, and D. Zhang, "FSIM: A feature similarity index for image quality assessment," *IEEE Trans. Image Process.*, vol. 20, no. 8, pp. 2378–2386, Aug. 2011.

[13] A. Liu, W. Lin, and M. Narwaria, "Image quality assessment based on gradient similarity," *IEEE Trans. Image Process.*, vol. 21, no. 4, pp. 1500–1512, Apr. 2012.

[14] W. Xue, L. Zhang, X. Mou, and A. C. Bovik, "Gradient magnitude similarity deviation: A highly efficient perceptual image quality index," *IEEE Trans. Image Process.*, vol. 23, no. 5, pp. 684–695, Feb. 2014.

[15] V. S. Petrovic and C. S. Xydeas, "Gradient-based multiresolution image fusion," *IEEE Trans. Image Process.*, vol. 13, no. 2, pp. 228–237, Feb. 2004.

[16] G. Chen, C. Yang, and S. Xie, "Gradient-based structural similarity for image quality assessment," in *Proc. IEEE Int. Conf. Image Process.*, Oct. 2006, pp. 2929–2932.

[17] J. Zhu and N. Wang, "Image quality assessment by visual gradient similarity," *IEEE Trans. Image Process.*, vol. 21, no. 3, pp. 919–933, Sep. 2011.

[18] W. Xue, X. Mou, L. Zhang, and A. C. Bovik, "Blind image quality assessment using Joint statistics of gradient magnitude and Laplacian features," *IEEE Trans. Image Process.*, vol. 23, no. 11, pp. 4850–4862, Aug. 2014.

[19] G. Cheng, J. Huang, C. Zhu, and Z. Liu, "Perceptual image quality assessment using a geometric structural distortion model," in *Proc. IEEE Int. Conf. Image Process.*, Sep. 2010, pp. 325–328.

[20] *VQEG* "Final Report From the Video Quality Experts Group on the Validation of Objective Models of Video Quality Assessment, Phase II," 2003. [Online]. Available: http://www.vqeg.org

[21] H. R. Sheikh and A. C. Bovik, "Image information and visual quality," *IEEE Trans. Image Process.*, vol. 15, no. 2, pp. 430–444, Feb. 2006.

[22] H. R. Sheikh, A. C. Bovik, and G. de Veciana, "An information fidelity creation for image quality assessment using natural scene statistics," *IEEE Trans. Image Process.*, vol. 14, no. 12, pp. 2117–2128, Dec. 2005.

[23] H. R. Sheikh, M. F. Sabir, and A. C. Bovik, "A statistical evaluation of recent full reference image quality assessment algorithms," *IEEE Trans. Image Process.*, vol. 15, no. 11, pp. 3440–3451, Nov. 2006.

[24] *Final Report From the Video Quality Experts Group on the Validation of Objective Models of Video Quality Assessment.* Aug. 2015. [Online]. Available: http://www.its.bldrdoc.gov/vqeg/vqeg-home.aspx

[25] Z. Wang and Q. Li, "Information content weighting for perceptual image quality assessment," *IEEE Trans. Image Process.*, vol. 20, no. 5, pp. 1185–1198, May 2011.

[26] D. M. Chandler and S. S. Hemami, "VSNR: A wavelet-based visual signal-to-noise ratio for natural images," *IEEE Trans. Image Process.*, vol. 16, no. 9, pp. 2284–2298, Sep. 2007.

[27] E. C. Larson and D. M. Chandler, "Most apparent distortion: Full-reference image quality assessment and the role of strategy," *J. Electron. Imag.*, vol. 19, no. 1, pp. 011006–1–011006-21, 2010.

[28] L. Zhang, Y. Shen, and H. Li, "VSI: A visual saliency-induced index for perceptual image quality assessment," *IEEE Trans. Image Process.*, vol. 23, no. 10, pp. 4270–4281, Aug. 2014.